LES OF FILM COOLING EFFICIENCY FOR DIFFERENT HOLE SHAPES

Peter Renze, Wolfgang Schröder, Matthias Meinke
Aerodynamisches Institut
Rheinisch Westfälische Technische Hochschule Aachen
Wüllnerstr. zw. 5 u. 7, D-52062 Aachen, Germany
p.renze@aia.rwth-aachen.de

ABSTRACT

Large-eddy simulations (LES) of film cooling flows are carried out at different hole shape geometries. The main thrust of this study is to contribute to the understanding of the impact of the hole shape on the mixing process of film cooling flows. A cooling fluid is injected from inclined drilling holes at $\alpha = 30^o$ into a turbulent boundary layer. Two different hole shapes are considered, a cylindrical geometry and a fan-shaped geometry that includes both a diffusor-like exit and a laidback expansion. The turbulent transport of heat and momentum has been investigated for the case of a cylindrical and a fan-shaped film cooling hole at a temperature gradient of $TR = 2.26$. The maxima of the turbulent shear stress and turbulent thermal transport of the jet-crossflow interaction are clearly reduced by the shaped jet hole. The instantaneous data show local ingestion of boundary layer fluid into the fan-shaped jet hole at the flow parameters considered in this study. The vortical structures inside the flow field and the driving mechanism of the momentum and heat exchange between the jet and the crossflow are identified and discussed.

INTRODUCTION

A high thermal efficiency in gas turbines engines is generally reached by high inlet gas temperatures. To protect the turbine components from the induced thermal stresses film cooling techniques are applied, that generate a thin film layer between the surface and the hot combustion gases.

Over the last decades few advancements have been introduced to this technology. The most significant one is the exit shaping of the film holes, that reduces the exit momentum of the jet and increases the surface coverage (Bunker 2005). The aim of the hole shape design is to maximize the cooling efficiency by the generation of a uniform, attached cooling film and to minimize the aerodynamic losses and the amount of process air. To meet these challenges, it is a must to completely understand the impact of the hole shape on the turbulent transport of momentum and heat in such flows.

Most investigations on film cooling hole shapes published in the literature are based on surface measurements only, without attention to the induced flow field. In the studies of Goldstein et al. (1974) or Makki and Jakubowski (1986) both cylindrical and widened injection holes have been investigated. The cylindrical configurations proved to be inferior against the shaped configurations and a higher overall cooling efficiency downstream of the injection was found. Especially the cooling efficiency at positions laterally displaced from the centerline was significantly improved.

Both numerical and experimental studies on this subject have been performed by Gartshore et al. (2001), who reported considerable changes in cooling efficiency despite rather small changes in the hole geometry. This study and most of the numerical investigations on this subject, e.g. by Brittingham and Leylek (2000), are based on the Reynolds-averaged Navier-Stokes equations (RANS).

However, since the jet-in-crossflow (JICF) problem is influenced by effects of wall-bounded and free turbulence, most standard turbulence models like zero-, one- or two-equation models fail to correctly predict the resulting flow field. For this reason, it is necessary to apply a more general numerical ansatz such as large-eddy simulation (LES) to investigate JICF problems. Large-eddy simulation have been performed, for instance, by Tyagi and Acharya (2003). An LES study that includes an accurate treatment of the incoming turbulent boundary layer and a plenum area was performed by Guo et al. (2006), who analyzed among other issues the impact of the inclination angle and the blowing ratio on the flow field. In recent studies Renze et al. (2006, 2007a) investigated an injection of a high-density cooling fluid into a low-density boundary layer flow using LES. The impact of the hole shape geometry on the film effectiveness has been studied in Renze et al. (2007b).

The present paper concentrates on the impact of the hole shaping on the turbulent transport of heat and momentum at realistic temperature conditions. It is the aim of this paper to contribute to the understanding of the physical mechanism, that leads to the rapid dispersion of film cooling jets and to explain in detail the benefits of shaped film cooling holes.

METHOD

The governing equations of the present LES are the filtered Navier-Stokes equations for compressible flows. The discretization of the governing equations is based on a mixed central-upwind AUSM (advective upstream splitting method) scheme using a centered 5-point low dissipation stencil to compute the pressure derivative in the convective fluxes. This scheme is described and validated by Meinke et al. (2002) and Rütten et al. (2005). Similar to the MILES approach as reported by Grinstein and Fureby (2002), the inherent dissipation of the numerical scheme serves as an implicit SGS model. The application of this method to the JICF problem and a detailed description of the boundary layer treatment has been published by Guo et al. (2006).

In the present work an independent spatially developing boundary layer simulation is performed to generate time-realistic inflow data at the beginning of the flat plate. The auxiliary flat plate flow simulation generates its own turbulent inflow data using the compressible rescaling method publisched by El-Askary et al. (2003) and Ewert et al. (2002). The rescaling method is a means of approximating the properties at the inlet via a similarity approach applied to the downstream solution.

FLOW CONFIGURATION

The domain of integration of the JICF simulation is shown in Fig. 1. The dashed lines mark the outer boundaries of the computational domain. The cooling fluid passes from a plenum through a 30^o streamwise inclined pipe into the boundary layer flow. The origin of the frame of reference is located at the jet hole center. The coordinates x, y, z represent the streamwise, normal, and spanwise direction.
To mimic the flow parameters in a gas turbine a cooling fluid is injected from a complete row of jets into a turbulent flat plate boundary layer at a Mach number $Ma = 0.2$ and a local Reynolds number of $Re_\infty = 400,000$ based on the length from the leading edge of the flat plate to the hole. The ratio of the local boundary layer thickness to the hole diameter is $\delta_0/D = 2$. The velocity, density, temperature and mass flux ratios are defined as

$$\begin{aligned} VR &= \frac{u_j}{u_\infty} = 0.28, \quad & DR &= \frac{\varrho_j}{\varrho_\infty} = 2.26, \\ TR &= \frac{T_j}{T_\infty} = 0.44, \quad & MR &= \frac{\varrho_j u_j}{\varrho_\infty u_\infty} = 0.63, \end{aligned} \tag{1}$$

where the subscripts $_j$ and $_\infty$ denote the jet and the mainstream. In the present study a standard cylindrical and a

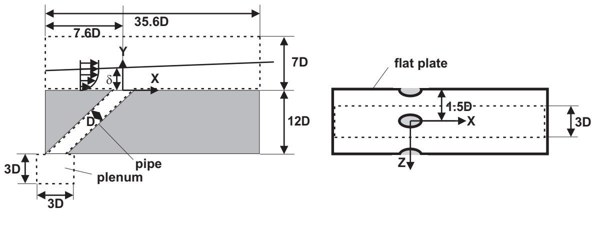

Figure 1: Schematic of the flow configuration in the x-y-plane (left) and the x-z-plane (right)

shaped jet hole are considered as sketched in Fig. 2. The geometry of the shaped exit hole is characterized by a lateral expansion (fan) and a laidback expansion in streamwise direction to achieve an increased lateral spreading of the cooling fluid and to further reduce the jet exit momentum in the wall-normal direction. The hole geometry is defined in Fig. 2.

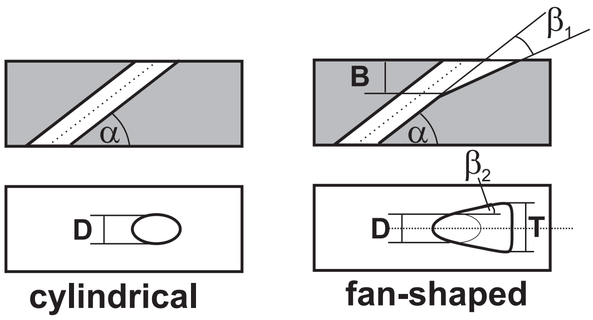

Figure 2: Schematic of the cylindrical and fan-shaped film cooling configuration with $B = 1.25D$, $T = 1.8D$, $\alpha = 30^o$, $\beta_1 = 8^o$, and $\beta_2 = 10^o$.

RESULTS

The discussion of the results consists of an analysis of the mean flow quantities, the turbulent shear stress and the turbulent heat transport for a cooling jet injected from two different hole shapes and a discussion of the vortical structures that govern the mixing process.

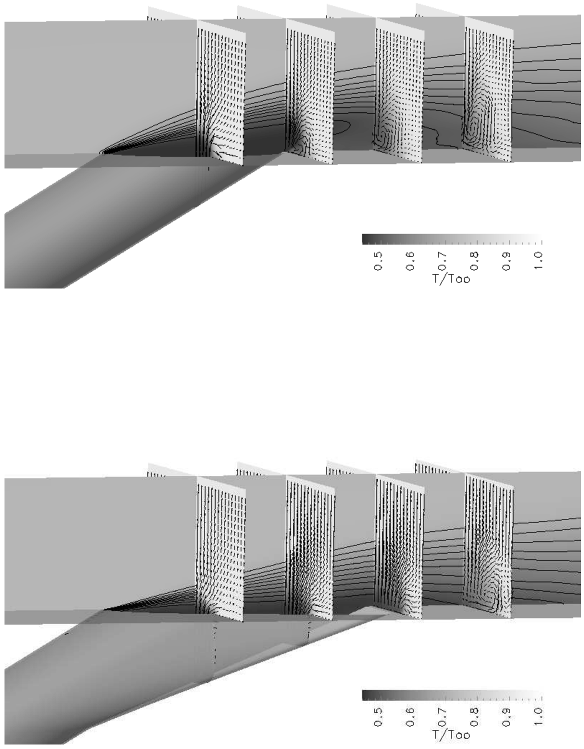

Figure 3: Contours of the averaged flow temperature T/T_∞ at several cross section and normalized vectors of the secondary velocity field. Top: cylindrical hole. Bottom: fan-shaped hole.

Mean Temperature and Velocity Field

The turbulent transport of heat and momentum in a film cooling flow is governed by the development of large-scale vortical structures. The differences in the hole shape geometry and the resulting impact on the jet exit momentum have a significant effect on the vortex dynamics and the turbulent mixing in the flow field. This will be discussed in the following with the help of averaged flow quantities, the turbulence statistics and the instantaneous coherent structures in the flow field.
The averaged temperature distribution is shown for both cases at different cross sections in Fig. 3. Vectors of the secondary velocity field complete the temperature contours. The cross section at $x/D = 0$ is located in the center of the cylindrical jet hole. The temperature contours demonstrate a deeper penetration of jet fluid into the crossflow for the cylindrical case at this axis location due to the higher jet exit momentum. For both cases the deflection of the boundary layer at the lateral edges of the jet holes can be observed. The mismatch in vertical momentum between crossflow and jet generates the counter-rotating roll-up of the boundary layer that will result in the counter-rotating vortex pair (CVP) downstream.
The position of $x/D = 1$ corresponds to the trailing edge for the cylindrical case. There, the beginning of a distinct wake region can be observed. The streamwise vortices of the CVP entrain crossflow fluid beneath the jet. Thus, the film cooling effectiveness is reduced and the flow temperature

at the plate is higher than in the jet center. The local temperature minimum in that cross section is lifted off the plate. At the same x-axis position in the fan-shaped case the cooling fluid passes through the fan and gets a stronger lateral velocity component. The vortices at the lateral edges are less developed.

At $x/D = 2$ the CVP is already fully developed in the cylindrical case. The jet flow temperature gets diffused following the development of the CVP. The local minimum is located between the CVP centers. To be more precise, it is slightly shifted in the wall-normal direction as the jet is lifted by the vortices. The maximum secondary velocities occur between the CVP centers and the flat plate, which is evident by the magnitude of the velocity vectors. In the fan-shaped case the trailing edge is reached at about $x/D = 2$. The trailing edge flow behavior is significantly altered. There is no distinct flow separation and the centers of the CVP are shifted in lateral direction. Although the flow temperature is already strongly diffused due to the low blowing ratio, the temperature distribution in lateral direction is more uniform and the film cooling effectiveness is improved. Further downstream at $x/D = 3$ the mixing between the jet fluid and the crossflow further reduces the local temperature minima. Downstream of the cylindrical jet hole the CVP is lifted, has grown in size and the centers approach each other. In the fan-shaped case a CVP is also evident at this position, although it is larger in size and the vorticity magnitude is smaller than in the cylindrical case, which is due to the weaker vertical and lateral momentum component induced by the fan. The resulting reduction of streamwise vorticity enhances the cooling efficiency. This flow behavior agrees well with the findings reported by Renze et al. (2007b).

Turbulent Shear Stress and Heat Transfer

The impact of the hole shaping on the turbulent transport of momentum and heat in the jet symmetry plane is shown in Fig. 4 for the cylindrical jet hole and in Fig. 5 for the fan-shaped jet hole. The distribution of the normal shear stress component $\overline{u'u'}/U_\infty^2$ is shown in Fig 4 a) and Fig. 5 a), respectively. In the cylindrical case three major zones of high turbulence levels can be observed. The first in the shear layer between the cooling jet and the crossflow, the second between the jet and wake at the trailing edge, and the third one in the mixing zone between $3 \leq x/D < 5$. Similar observations have been reported, e.g., by Peterson and Plesniak (2004), who analyzed the turbulent Reynolds stress components determined by PIV measurements at cylindrical jet holes. The areas of high turbulence correspond to regions where large velocity gradients occur in the mean flow field.

In case of the fan-shaped jet hole the first zone of high turbulence between the jet and the crossflow is less pronounced. It does not penetrate as deep into the crossflow due to the reduced exit momentum and the peak values are reduced. The high shear stress between the jet and the wake observed in the cylindrical case does not occur in this configuration, because there is no significant recirculation region. In the third zone between $3 \leq x/D < 5$, i.e. downstream of the jet hole, high levels of turbulence are evident, but the peak values of $\overline{u'u'}/U_\infty^2$ are reduced from 0.035 to 0.025. In Thole et al. (1998) a similar reduction of turbulence level in this region was reported for a fan-shaped jet hole. Furthermore, inside the jet hole high levels of turbulence can be identified, that result from vortical structures generated inside the jet exit. These vortical structures have been discussed in Renze et al. (2007b). They lead to a weak ingestion of hot boundary layer fluid, that will be addressed later.

The distribution of the turbulent shear stress component $\overline{u'v'}/U_\infty^2$ is shown in the part b) of Fig 4 and Fig. 5. This turbulent shear stress component is directly connected to the turbulent transport of momentum in the streamwise and wall-normal direction. The peak level of $\overline{u'v'}/U_\infty^2$ in the undisturbed turbulent boundary layer is about -0.002. The turbulence level is negative due to the large positive mean velocity gradient in the flow field. In the mixing zone between the jet and the mainstream this level can reach values of $\overline{u'v'}/U_\infty^2 = -0.008$ directly over the jet hole and in the zone of high turbulence between $3 \leq x/D < 5$, i.e., the mixing is much more vigorous than in an ordinary turbulent boundary layer flow or a turbulent free jet. This corresponds to the findings of a study reported by Kohli and Bogard (2005) based on LDV measurements.

If the distribution of turbulent shear stress $\overline{u'v'}/U_\infty^2$ is compared to the fan-shaped case, it is evident, that the vigorous turbulent mixing is reduced. Directly above the jet hole exit and in the jet-mainstream interface between $3 \leq x/D < 5$ the peak levels reach only a magnitude of $\overline{u'v'}/U_\infty^2 = -0.0062$ and this region is more localized than in the cylindrical case. This is substantial since the mean velocity gradient is as steep as in the cylindrical case, especially over the jet hole. The high turbulent shear stress in these regions is due to strong vortex shedding that originates from the leading edge of the jet hole. These shear layer vortices can be observed in Fig. 3 and Fig. 7. Thus, the reduced turbulent shear stress $\overline{u'v'}/U_\infty^2$ in the fan-shaped case has to be due to weaker shear layer vortices in the mixing zone between the jet and the crossflow.

Vortical Structures in the Instantantaneous Flow Field

Contours of the fluctuating temperature $\sqrt{\overline{T'T'}}/T_\infty$ is shown in the part c) of Fig. 4 and Fig. 5 for both geometry cases. High fluctuations in the temperature field are clearly connected to the large gradients in the mean temperature field, that is shown in Fig. 3. The strong mixing is evident in the initial interface between the jet and the crossflow starting at the leading edge of the film cooling holes. The dispersion of the jet fluid in these mixing zones reduces the peak fluctuation levels very rapidly. On the one hand, the comparison of both cases shows again a deeper penetration of the mixing zone in wall normal direction for the cylindrical case. On the other hand, the mixing region reaches into the jet hole in the fan-shaped case and an ingestion of hot mainstream fluid at the leading edge and the laidback part of the exit fan is visible.

The amount of turbulent thermal transport is crucial for the prediction of the thermal dispersion of the jet fluid and thus, for the film cooling effectiveness. The predicted turbulent thermal transport $\overline{u'T'}/(U_\infty T_\infty)$ is shown in Fig. 4 d) for the cylindrical case and Fig. 5 d) for the fan-shaped case. Negative peak values of $\overline{u'T'}/(U_\infty T_\infty) = -0.005$ characterize the mixing in the recirculation region of the cylindrical jet, whereas the same negative level is evident inside the fan-shaped jet hole directly at the trailing edge, where the fluid ingestion is observed. The positive peak levels occur at the blocked region of the jet near the leading edge for both cases. This zone is more pronounced for the cylindrical case indicating higher thermal transport in this initial mixing zone.

In Fig. 6 distribution of the normal Reynolds stress components $\overline{u'u'}/U_\infty^2$, $\overline{v'v'}/U_\infty^2$ and $\overline{w'w'}/U_\infty^2$ are shown in a cross

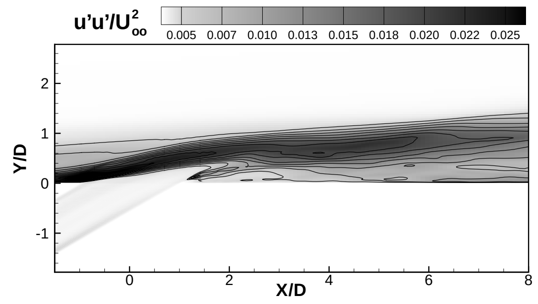

a)

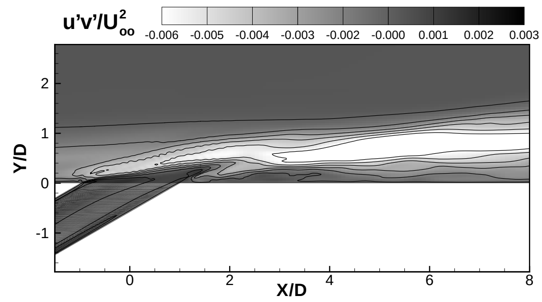

b)

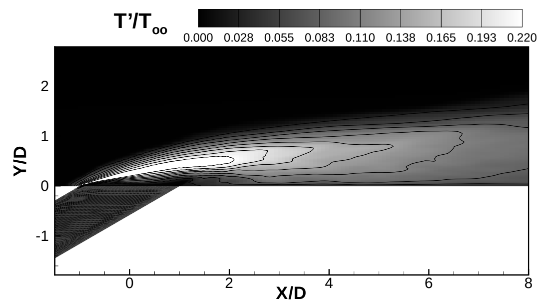

c)

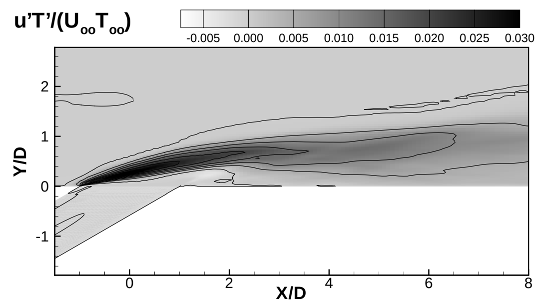

d)

Figure 4: Cylindrical jet hole: Contours of shear stress and thermal transport in the jet symmetry plane, a) $\overline{u'u'}/U_\infty^2$, b) $\overline{u'v'}/U_\infty^2$, c) $\sqrt{\overline{T'T'}}/T_\infty$, d) $\overline{u'T'}/(U_\infty T_\infty)$.

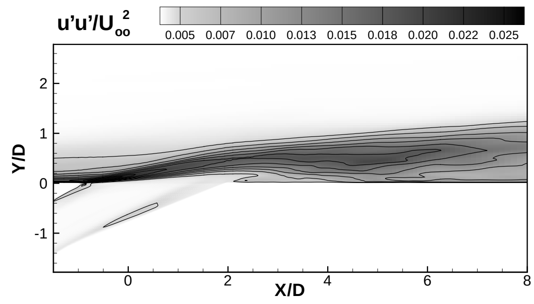

a)

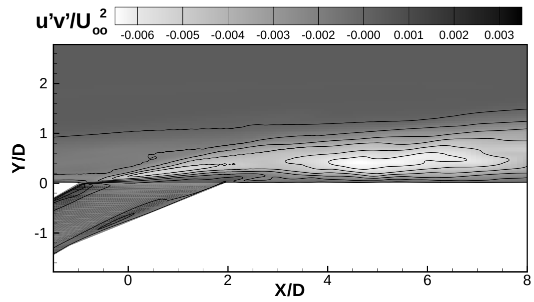

b)

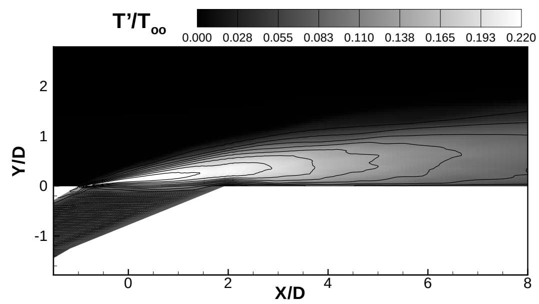

c)

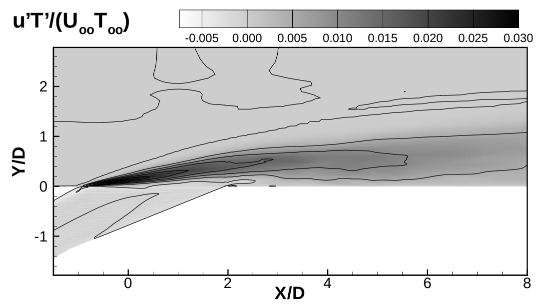

d)

Figure 5: Fan-shaped jet hole: Contours of shear stress and thermal transport in the jet symmetry plane, a) $\overline{u'u'}/U_\infty^2$, b) $\overline{u'v'}/U_\infty^2$, c) $\sqrt{\overline{T'T'}}/T_\infty$, d) $\overline{u'T'}/(U_\infty T_\infty)$.

section at $x/D = 4$ for both geometries. This cross section is located downstream of the jet exit in the mixing zone for both cases. At this low blowing ratio the jet-crossflow interaction occurs in the lower parts of the turbulent boundary layer and is clearly characterized by anisotropy as was shown by Guo et al. (2006). This is evident in Fig. 6. The normal Reynolds stress components in the lateral and wall-normal direction reach only half of the maximum level of the streamwise component. The presence of the wall damps the wall-normal velocity fluctuations and a higher amount of anisotropy than in a free jet mixing case is to be expected. A comparison of the Reynolds stresses for both geometries shows an overall reduction of the turbulence levels for the fan-shaped case. The maxima are shifted in the direction of the wall as the vertical jet exit momentum is reduced.
The CVP has a larger expansion in lateral direction for the fan-shaped case as shown in Fig. 3. Consequently, the Reynolds stresses are more pronounced in lateral direction. This has a significant impact on the film cooling effectiveness as the lateral coverage of the plate is improved and the thermal transport in wall-normal direction is reduced.
In the preceding discussion of the turbulent transport of momentum and heat in the film cooling flow field the important role of the formation of vortical structures in the shear layer between the jet and the crossflow was addressed. To emphasize the significant differences in the formation of the shear layer vortices and the counter-rotating vortex pair for both cases the instantaneous coherent structures are discussed in the following.
In Fig. 7 vortical structures are indicated by the λ_2 criterion, that was proposed by Jeong and Hussain (1995). Here, the same small negative value is chosen for both geometries. The local temperature distribution is mapped on the vortical structures. A cut plane at $z/D = 0$ limits the λ_2-contours to give insight on the instantaneous temperature distribution shown in a plane adjacent to the wall surface.
The vortices upstream of the jet hole represent the coherent structures of the turbulent boundary layer flow, that enters

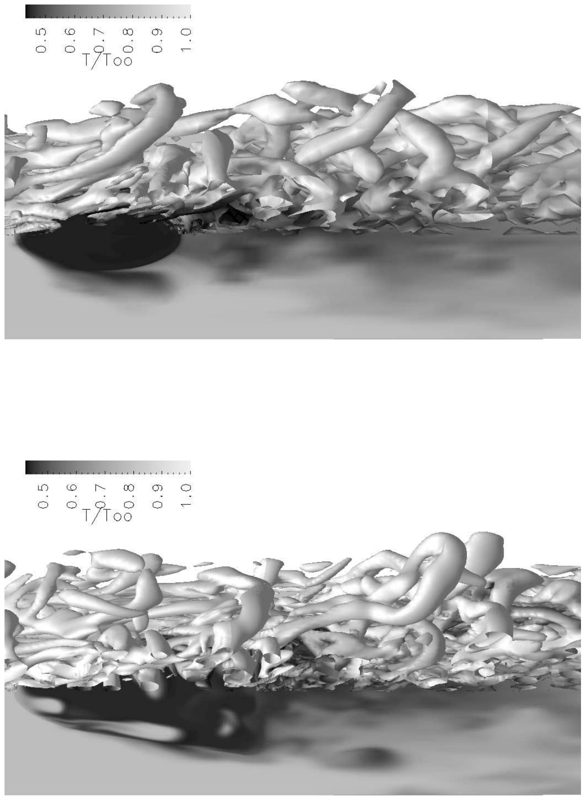

Figure 7: Coherent structures of the instantaneous flow field indicated by the λ_2 criterion and mapped temperature distribution T/T_∞. Top: cylindrical hole. Bottom: fan-shaped hole.

the computational domain a few diameters upstream of the jet hole. At this low-Mach number problem the temperature in the boundary layer nearly equals the mainstream temperature. At the leading edge of the film hole the jet fluid is initially blocked by the crossflow. Shear layer vortices are generated additional to the inherent structures in the lifted turbulent boundary layer. These shear layer vortices are convected downstream of the jet exit. They are wrapped around the jet fluid. The wall-normal velocity gradient leads to a difference in the convection speed along the vortices. This mechanism generates the hairpin-like structures around the jet core as reported by Tyagi and Acharya (2003). The vortices associated with the legs of these hairpin-like structures are oriented in streamwise direction and can be noted as the CVP in the averaged flow field. The heads of the hairpin-like structures are located between the jet and the crossflow in the symmetry plane and contribute to the high turbulent shear stress in this region. The reduced exit momentum and the higher lateral momentum component in the fan-shaped case reduces the strength of this mixing process.
In the case of the cylindrical jet hole the recirculation region with its complex wake vortices is evident. In this area mainstream fluid is entrained in a swirling motion beneath the cooling jet and the film effectiveness is severely decreased. Due to the greater lateral spreading and the reduced vertical exit momentum this cannot be observed in the fan-shaped case.
The impact of the reduced exit momentum on the dispersion

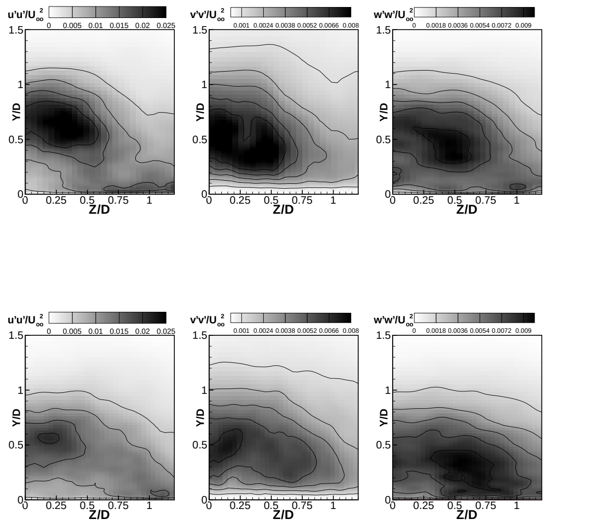

Figure 6: Distribution of the normal Reynolds stress components $\overline{u'u'}$, $\overline{v'v'}$ and $\overline{w'w'}$ scaled by the mainstream velocity U_∞ in a cross section at $x/D = 4$. Top: cylindrical hole. Bottom: fan-shaped hole.

of the cooling fluid near the flat plate surface is demonstrated in Fig. 7. The higher exit momentum at the cylindrical jet hole leads to a roll-up of the boundary layer fluid at the lateral edges. This motion entrains cooling fluid in lateral direction. The strong streamwise momentum of the mainstream convects this fluid downstream over the plate surface as is evident by the streak of low temperature in Fig. 7 (top). In the fan-shaped case this entrainment is weaker due to the reduced exit momentum. Here, the boundary layer flow passes almost horizontally over the leading edge and boundary layer fluid is entrained into the jet hole. Thus, the mixing zone extends into the hole as shown in Fig. 5. The possibility of fluid ingestion for this kind of shaped hole at low blowing ratios is briefly discussed in Bunker (2005), but no detrimental effect on the lifespan of the engine components is reported by the gas turbine manufacturers. Nevertheless, these instantaneous flow phenomena have to be considered in the design process of new film cooling configurations.

CONCLUSION

Large-eddy simulations are performed to investigate the impact of hole shaping on the turbulent transport of momentum and heat in film cooling flows. The main thrust of this study is to contribute to the understanding of the impact of the hole shape on the mixing process of film cooling flows. The turbulent transport of heat and momentum has been investigated for the case of a cylindrical and a fan-shaped film cooling hole at a temperature gradient of $TR = 2.26$.
The peak levels of the turbulent shear stress occur in the mixing zone between the jet and the crossflow directly over the film hole and between $3 \leq x/D < 5$. The peak levels are clearly reduced in the jet-mainstream interface for the fan-shaped jet hole. The thermal transport has been evaluated analyzing the fluctuations of the flow temperature and the turbulent heat flux. While the fluctuation are of the same magnitude in the shear layers, the turbulent heat flux is reduced in the fan-shaped case.
The reduction in turbulent heat transport has been discussed on the basis of the vortical structures in the instantaneous flow field. The detrimental effect of the recirculation region at the leading edge of the cylindrical jet hole and the weaker CVP downstream of the fan-shaped jet hole are demonstrated.

ACKNOWLEDGMENTS

The support of this research by the Deutsche Forschungsgemeinschaft (DFG) in the frame of SFB 561 is gratefully acknowledged. The simulations were run on the NEC-SX8 cluster at the High Performance Computing Center Stuttgart (HLRS) of the University of Stuttgart.

REFERENCES

Brittingham, R. A. and Leylek, J. H. 2000. "A detailed analysis of film cooling physics: Part IV: Compound-angle injection with shaped holes". *ASME J. Turbomach.*, Vol. 122, No. 1, pp. 133–145.

Bunker, R. S. 2005. "A review of shaped hole turbine film-cooling technology". *ASME J. Heat Transfer*, Vol. 127, pp. 441–453.

El-Askary, W.A., Schröder, W., and Meinke, M. 2003. "LES of compressible wall-bounded flows". AIAA Paper 2003–3554.

Ewert, R., Schröder, W., Meinke, M., and El-Askary, W.A. 2002. "LES as a basis to determine sound emission". AIAA Paper 2002–0568.

Gartshore, I., Salcudean, M., and Hassan, I. 2001. "Film Cooling Injection Hole Geometry: Hole Shape Comparison for Compound Cooling Orientation". *AIAA J.*, Vol. 39, No. 8, pp. 1493 – 1499.

Goldstein, R. J., Eckert, E. R. G., and Burggraf, F. 1974. "Effects of hole geometry and density on three-dimensional film cooling". *Int. J. Heat Mass Transfer*, Vol. 17, No. 5, pp. 595 – 607.

Grinstein, F. F. and Fureby, C. 2002. "Recent progress on MILES for high Reynolds number flows". *J. Fluids Eng.*, Vol. 124, pp. 848–861.

Guo, X., Meinke, M., and Schröder, W. 2006. "Large-eddy simulations of film cooling flows". *Computers & Fluids*, Vol. 35, pp. 587–606.

Jeong, J. and Hussain, F. 1995. "On the identification of a vortex". *J. Fluid Mech.*, Vol. 285, pp. 69–94.

Kohli, A. and Bogard, D.G. 2005. "Turbulent transport in film cooling flows". *ASME J. Heat Transfer*, Vol. 127, No. 5, pp. 513–520.

Makki, Y. H. and Jakubowski, G.S. 1986. "An experimental study of film cooling from diffused trapezoidal shaped holes". AIAA Paper 86-1326.

Meinke, M., Schröder, W., Krause, E., and Rister, Th. 2002. "A comparison of second- and sixth-order methods for large-eddy simulations". *Computers & Fluids*, Vol. 31, pp. 695–718.

Peterson, S. D. and Plesniak, M. W. 2004. "Evolution of jets emanating from short holes into crossflow". *J. Fluid Mech.*, Vol. 503, pp. 57–91.

Renze, P., Schröder, W., and Meinke, M. 2006. "Large-eddy simulation of film cooling flows with variable density jets". *submitted to Flow, Turbulence and Combustion.*

Renze, P., Meinke, M., and Schröder, W. 2007a. "Large-eddy simulation of film cooling at density gradients". *submitted to Int. J. Heat Fluid Flow.*

Renze, P., Schröder, W., and Meinke, M. 2007b. "Hole shape comparison for film cooling flows using large-eddy simulations". AIAA Paper 2007-0927.

Rütten, X., Schröder, W., and Meinke, M. 2005. "Large-eddy simulation of low frequency oscillations of the Dean vortices in turbulent pipe bend flows". *Phys. Fluids*, Vol. 17, pp. 035107.1–035107.11.

Thole, K., Gritsch, M., Schulz, A., and Wittig, S. 1998. "Flow field measurements for film-cooling holes with expanded exits". *ASME J. Turbomach.*, Vol. 120, pp. 327–336.

Tyagi, M. and Acharya, S. 2003. "Large Eddy Simulation of Film Cooling Flow from an Inclined Cylindrical Jet". *ASME J. Turbomach.*, Vol. 125, No. 4, pp. 734–742.